Eur. Phys. J. B (2009)
DOI: 10.1140/epjb/e2009-00282-4

THE EUROPEAN PHYSICAL JOURNAL B

Regular Article

A numerical study of energy transfer mechanisms in materials following irradiation by swift heavy ions

P. Baril, L.J. Lewis[a], and S. Roorda[b]

Département de Physique et Regroupement Québécois sur les Matériaux de Pointe (RQMP), Université de Montréal, C.P. 6128, Succursale Centre-Ville, Montréal, Québec, H3C 3J7, Canada

Received 10 June 2009 / Received in final form 2 July 2009
Published online 13 August 2009 –

Abstract. Swift heavy ions interact with electrons in materials and this may yield permanent atomic displacements; the energy transfer mechanisms that bring electronic excitations into atomic motion are not fully understood, and are generally discussed in terms of two theories, viz. Coulomb explosion and heat exchange between excited electrons and atoms, which is limited by electron-phonon coupling. We address this problem for a "generic" material using a semi-classical numerical approach where the dynamics of the evolving electron density is calculated by using molecular dynamics simulations applied to pseudo-electrons. The forces exerted on the nuclei are then used to calculated the trajectories of the nuclei. From the temporal evolution of the atomic kinetic energy, we find that the energy transfer between the electrons and the nuclei can be divided in two parts. First, a Coulomb heating starts the motion of the atoms by giving them a radial speed; this process differs from Coulomb explosion because the atoms are not displaced over interatomic distances. Second, a thermal energy transfer, as described in linear transport theory, takes place. Our study thus confirms the domination of thermal energy exchange mechanisms over Coulomb explosion models.

PACS. 61.80.Az Theory and models of radiation effects – 63.20.kd Phonon-electron interactions

1 Introduction

In the study of the interactions of ions with matter, two energy regimes are of interest: slow ions ($E <$ keV/amu), where the interactions essentially consist of binary collisions between the projectiles and the target atoms, and fast, or "swift", ions ($E \sim$ MeV/amu), where the interactions initially proceed by the excitation of the electrons, which eventually transfer their energy to the lattice. In both cases, significant damage can result, ranging from simple point defects to extended amorphous tracks [1–4].

A full theoretical understanding of the energy transfer processes during the swift heavy ion irradiation of solid materials is far from having been achieved. The ions are slowed down so violently that they deposit keV's of energy per nm along their trajectories [5]. In this regime, the cross-section for atomic collisions (which can lead to collisions cascades) is so small that they can be ignored and the ions are slowed down mostly by interactions with electrons in the solid [4]. Thus the target contains a large local density of highly excited electrons, with some form of cylindrical symmetry reflecting the shape of the ion trajectories. These excited electrons transfer their energy to the atoms making up the solid target; how fast, how localized, and by which mechanism the energy transfer takes place remains far from being fully understood.

At least two radically different energy transfer mechanisms have been proposed [6–8], and these are not mutually exclusive as they may take place on different time windows. One is "Coulomb explosion": a region along the centre of the ion trajectory becomes partly or completely denuded of electrons and, as a result, the remaining atoms experience a Coulomb repulsion causing them to be accelerated radially outward until their charges are (again) screened by the electrons. The associated energy transfer mechanism is therefore of Coulombic origin. It is not know how fast the screening re-establishes itself, in part because such a large fraction of the electrons is so highly excited. The "explosion" leaves many defects behind, including, possibly, an elongated amorphous region [9]. Another mechanism is sometimes referred to as the "thermal spike": the excited electrons transfer their energy by electron-phonon coupling to the lattice atoms [4,10], and this leads to a localized high-temperature region (and possibly local melting along the ion track). According to this process, the energy transfer proceeds by random

[a] e-mail: laurent.lewis@UMontreal.ca
[b] e-mail: sjoerd.roorda@UMontreal.ca

collisions. However, electron-phonon couplings for far-from-equilibrium systems, as is the case during swift heavy ion irradiation, are difficult to estimate. Other theories include shock waves [11] and lattice relaxation [12].

The lack of understanding of these energy transfer processes needs to be addressed, because several surprising observations have been made on materials under swift heavy ion irradiation. For example, amorphous materials exhibit the hammering effect, whereby an irradiated thin film becomes thinner and wider, as if each ion acts like a little hammer [13]. Similarly, the irradiation of materials with off-axis ions can lead to lateral transport of target surface layers in the direction of the component of the ion velocity parallel to the sample surface [14,15]. In many materials, the passage of swift heavy ions leaves latent tracks that cannot be detected directly but can be revealed because they are vulnerable to chemical attack by etchants or solvents (depending on the material) [16]. And curiously, spherical metal nanoparticles embedded in an amorphous matrix can be deformed into nano-rods, aligned along the direction of the incident ions [17]. A consensus has not been reached on a full explanation of these phenomena, and an improved understanding of the behaviour of a high density of highly excited electrons would be very helpful. In addition, a new theoretical approach is needed to understand the damage created by ion irradiation of substrates such as carbon nanotubes or sheets of graphene [18] that are thinner than the radius of the ion track in the corresponding bulk material.

A full ab initio description of any of those experimental observations is an unmanageable task for a number of reasons. Among them, the time scales to be treated range from the fs regime (roughly the time it takes the ion to travel a nm) to full seconds (the time scale that can be involved in point defect recombination). Also, the core electrons can become excited and need to be included in the calculations, imposing a large computational workload.

We present, in this article, the results of a numerical study of the passage of swift ions in matter with a view of identifying the chain of events leading to the transfer of energy to the atoms and eventual damage to the target. Our approach is based on classical molecular-dynamics (MD) simulations, but the electrons are incorporated in an ad hoc, quasi ab initio (or semi-empirical) manner. Thus, electronic effects can be fully taken into account and the energy transfer mechanisms need not be assumed a priori as in other approaches [4,10]. Our model is "generic", i.e., it does not describe a particular material, though it eventually could. Anticipating our results, we find that the energy transfer from the swift ions to the lattice proceeds along two different routes: first, radial Coulomb heating, then purely thermal processes. The present study only considers energy transfer processes between the highly excited electrons and the atomic lattice; we have not studied subsequent changes to the lattice (such as amorphization, deformation, etc.) which would required MD calculations over much longer time scales to be performed. We begin by presenting our model and discussing the theoretical background.

2 Model and computational details

The problem of a swift ion interacting with a material is studied here using classical MD simulations whereby the trajectories of all the particles in the system are followed in time by integrating their equations of motion under an appropriate representation of the total energy of the system (see below) [19]. The electrons play an essential role in the present case and therefore have to be explicitly considered. We do this using the semi-classical approach proposed by Mijoule et al. [20] which is based on a hydrodynamic formulation of quantum mechanics (Madelung equations) [21]. The approach is properly modified to duly take into account the boundary conditions for our particular system, viz. periodic. In summary, the atoms are assumed to consist of charged nuclei ('n') and electrons, and the latter are subdivided into N pseudo-electrons (PE), each of charge e/N and mass m_e/N, where e and m_e are the charge and the mass of one electron, respectively. The PEs are treated in a classical manner, and their equations of motion are followed, just as with the nuclei, using MD, but with a much smaller time step. With this procedure, the number of electrons can be changed at will, and the electronic density is properly described as we will see.

The interactions between all particles, viz. n-n, n-PE, and PE-PE, are Coulombic. For the particular case of n-PE interactions, however, the Coulomb potential has to be modified at short range to prevent the PEs from collapsing onto the nuclei. This is done by introducing a repulsive term at short distances; more specifically, the force (which is the quantity of interest in MD simulations) is written

$$\boldsymbol{f}_{ne}(\boldsymbol{r}) = Qq\left[\frac{2(1+\alpha r)e^{-\alpha r}-1}{r^2}\right]\hat{r}. \tag{1}$$

The parameter α sets the minimum of the potential energy, i.e., it fixes the size of the distribution of electrons around the nuclei. As for the PE-PE interactions, also Coulombic, they are smoothed using an error function to ensure that the force between atoms is attractive:

$$\boldsymbol{f}_{ee} = \frac{\mathrm{erf}(\gamma r)}{r^2}\hat{r}, \tag{2}$$

where γ corresponds to the distance from which the force becomes purely Coulombic.

Coulomb forces are long range and, because we use periodic boundary conditions, have to be handled with care. These are normally calculated using the Ewald summation technique. This method however is quite slow. Following Fennell and Gezelter [22], we cut and shift the forces, instead, a procedure which is equivalent to the Ewald summation for a proper choice of cutoff radius. Fennell and Gezelter indicate that this should be larger than 9 Å [22]; we used 12 Å.

The starting point configuration of the target is constructed as follows. First, the atoms, which consist of a nucleus of mass m and a single charge e (see below), are placed on the nodes of a face-centered cubic (FCC) lattice – here $10 \times 10 \times 6$ unit cells –, the equilibrium structure for this model. (The lattice parameter is discussed

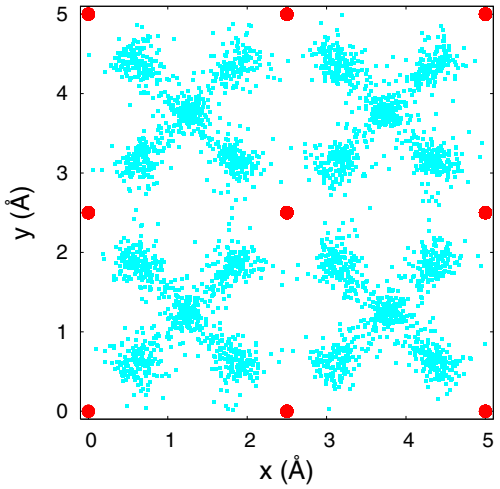

Fig. 1. (Color online) Two-dimensional projection of the initial state of the system (the lattice is FCC). Blue squares and red circles represent the PEs and the nuclei, respectively.

below.) The PEs are then randomly distributed in the simulation volume and a steepest-decent relaxation calculation (at 0 K) is carried out on their positions in order to minimize the total energy of the system. A typical configuration obtained in this way is illustrated in Figure 1, where the coordinates of all particles have been folded back into a single unit cell and projected onto the (x, y) plane, that is normal to the direction of incidence of the ion.

The values of the various parameters entering the model are somewhat arbitrary and are chosen so as to provide a qualitatively correct description of a "generic" material. Thus, our model does not represent a particular system – it could be extended to do this – but, rather, is designed to possess the physical ingredients which are essential to a proper description of the interaction of a swift ion with matter. For the simulations described below, each electron was assumed to consist of 4 PEs, which provides a reasonable electronic density and a computationally manageable system. The distribution of electrons can be seen in Figure 1 where "bonds" are clearly visible. Thus, even though the structure is close-packed, this system has electronic features that can be associated to covalent crystals or semiconductors. These characteristics should not be taken at face value, however, and they need not to as they are not determinant to a proper description of the interaction of swift ions with matter at this level of understanding and approximation.

For the other parameters, we set $\gamma = 0.228$ Å^{-1} and $\alpha = 1.20$ Å^{-1} which yield a qualitatively correct behavior. With these choices, the lattice constant is found to be 5.0 Å, which is quite appropriate for an FCC material. The mass of the nuclei was set to 0.01 amu; this evidently very small value is chosen to accelerate the dynamics of the ions. Indeed, the timescale of the problem is largely determined by the dynamics of the electrons, which is much faster than the nuclei's; hence this choice is not detrimental to our calculations but does improve efficiency considerably. To make contact with "real" units, we note that the ion relaxation times vary roughly linearly with the ion mass; since the mass of a typical ion would be ∼10 amu, this means that the time is compressed by a factor of roughly 10^3. In view of this, time will be expressed in what follows in units of t_u, which is about 1 ps for physically appropriate model parameters.

In order to validate our model, we calculated the potential energy of an additional particle in the solid and found that it followed very closely the predictions of the Thomas-Fermi theory, i.e., screening is properly taken into account. We also examined energy transport properties, which were found to behave correctly. Energy transport between electrons and thermal energy exchange between species are well predicted by first-order transport theory. Finally, we calculated the melting temperature of the system and found it to be about 0.15 eV, i.e., ∼1800 K.

Other details of the model are as follows. As noted earlier, the system size was set to $10 \times 10 \times 6$ FCC unit cells – that is 2400 atoms and 9600 PEs for a total of 12 000 MD particles – which we found is sufficiently large to ensure converged results. We employ periodic boundary conditions to mimic an infinite system; however, in order to eliminate the effects of periodic images on the single ion problem we study here, and to limit the energy fluctuations at the beginning of the process, when PEs reach an x or y boundary with an energy larger than 0.3 eV, their energy is removed and reset to 0. The equations of motion are integrated using the velocity Verlet algorithm with a timestep of 10^{-18} s. Finally, the point of impact of the ion is chosen to be in the middle of the simulation cell; we have verified that the results do not depend on this choice since there are no "head-on" collisions between the incoming ion and the lattice nuclei, as we discuss next.

To simulate the interactions of a fast ion with the electrons in the target, we have to know the way the electrons are affected by a swift ion. The program CASP (Convolution Approximation for Swift Particles), developed by Grande and Schiwietz [23,24], gives this information for specific ions in specific materials. CASP considers the electric field produced by a fast ion as a perturbation to the electronic wave functions in the solid, allowing the energy transfer to be computed as a function of the impact parameter. We used this program to obtain a general rule for the electronic excitations, based on simulations with different ions on different targets. From these calculations, we find that only external shell electrons are affected for swift ions and that only those very near the impact trajectory absorb a significant amount of energy. Typical CASP simulations are well represented by the following Gaussian distribution for the energy absorbed by the electrons as a function of the radial distance ρ from the impact line:

$$S_e(\rho) = Q_e \frac{a^3}{4\pi\sigma^2} \exp\left(-\frac{\rho^2}{\sigma^2}\right), \qquad (3)$$

with $\sigma = 1.7$ Å. For swift ions, the electronic excitations are much more important than the direct transfer to the atoms so that Q_e in effect represents the stopping power of the incident ions. This quantity can be measured

experimentally; it usually lies in the range 1–100 keV/nm (10^2–10^4 eV/Å). Using this result, we set the radial speed of the PEs to:

$$v_e^{\rho}(\rho) = -\sqrt{\frac{2S_e(\rho)}{m_e}}. \tag{4}$$

The energy to the PEs is introduced in one shot at the beginning of the simulation. This is justified by the fact that the impact ion swiftly travels through the target. Several values of the stopping power, from 16 to 2000 eV/Å, were considered.

3 Theoretical background

The energy transfer mechanisms can be identified by examining the temporal evolution of the kinetic energy of the nuclei, $K_n(t)$; indeed, the energy gain is much faster in the case of a Coulomb explosion than in the case of thermal transfer. We briefly review the two mechanisms here in order to provide an appropriate reference frame for understanding our simulations.

According to the "thermal spike" model, the electrons are excited by the swift ion, thermalize, and their energy is subsequently transferred to the atoms by random collisions [4]. The kinetic energy of the nuclei therefore evolves following linear transport theory. Considering the electrons and the nuclei as two distinct, uniform fluids of constant density and zero net velocity, linearly coupled via their temperatures, the evolution of the mean temperatures of the two fluids is given by:

$$\begin{aligned} C_e \frac{\partial \overline{T}_e}{\partial t} &= -G(\overline{T}_e - \overline{T}_n), \\ C_n \frac{\partial \overline{T}_n}{\partial t} &= G(\overline{T}_e - \overline{T}_n). \end{aligned} \tag{5}$$

Here, C_e and C_n are the specific heats of the two systems, $\overline{T}_e$ and $\overline{T}_n$ are the temperature of the electrons and the nuclei, respectively, and G represents the coupling between the two fluids. Under the above assumptions (uniform fluids, constant density and zero net velocity), the temperatures are related to the mean kinetic energies by $\overline{K}_i = C_i \overline{T}_i$. Solving those equations, it can be shown that the mean kinetic energy of the nuclei depends exponentially on time:

$$\overline{K}_n(t) = K_1 \exp(-t/\tau_{ne}) + K_2, \tag{6}$$

where K_1 and K_2 are constants fixed by the initial conditions of the two fluids, and τ_{ne} is the relaxation time for heat exchange between them, which depends on the strength of the coupling. We may go one step further by considering the potential energy as another fluid, representing the spatial degrees of freedom. This brings about an additional exponential term in equation (6); we found however that this correction is minor and that equation (6) adequately describes the thermal processes that we simulate, with a relaxation time of about 13 t_u.

The Coulomb explosion model is based on the fact that electrons are ejected from the center of the impact track, causing a net positive charge which in turn causes the nuclei in the affected region to expel one another. As the nuclei are displaced over several interatomic distances, the damaged zone effectively becomes depleted. The gain in energy of the nuclei can be calculated by considering the impact of an electrically charged cylinder on the nuclei. The cylinder's linear density of charge λ decays exponentially with time, with characteristic screening time τ_r:

$$\lambda(t) = \lambda_0 \exp(-t/\tau_r), \tag{7}$$

where λ_0 is the initial charge density. From this charge we can determine the forces acting on the nuclei, which can be integrated numerically to yield the velocities and energies of the nuclei. An analytical solution can also be obtained if the displacements of the nuclei are assumed to be small; this approximation is evidently in contradiction with the Coulomb explosion model but will prove to be useful later for interpreting our results. We thus find:

$$K_n(t) = K_3[\beta - \exp(-t/\tau_r)]^2, \tag{8}$$

where β is given by the initial velocity of the atoms and K_3 depends on λ_0 and τ_r.

As we will see below, equations (6) and (8) for the temporal evolution of the kinetic energy of the electrons in the two models provide a proper criterion for identifying the energy transfer mechanisms.

4 Results and discussion

4.1 State of the target after the impact

We begin the presentation of our results by describing the state of the target during the moments that follow the impact. This will be helpful for identifying the important phases the system goes through as a function of time, discussed in the next section.

Figure 2 shows the radial, lateral, and vertical (i.e., z) components of the kinetic energy of the electrons as a function of time. (In this and other figures, the energy loss is set to $Q_e = 80$ eV/Å unless otherwise indicated.) Four stages of evolution can be identified. First, at very short time (stage I), the radial component possesses a very high value which corresponds to the radial speed imposed on the electrons to simulate the effect of the swift ion, as discussed earlier. This energy has not yet been transferred to the other two components, which are close to zero (note the log scale). In stage II, the radial component decreases rapidly while the lateral and vertical components gain intensity. This rapid drop corresponds exactly to the loss of energy from the fast electrons crossing the boundaries of the simulation cell, demonstrating that the electrons are very rapidly evicted – in about 0.2 t_u – from the central region of the target. Most of the energy initially introduced in the system is evacuated in this way. Equilibration proceeds during stage III and is completed in stage IV, that

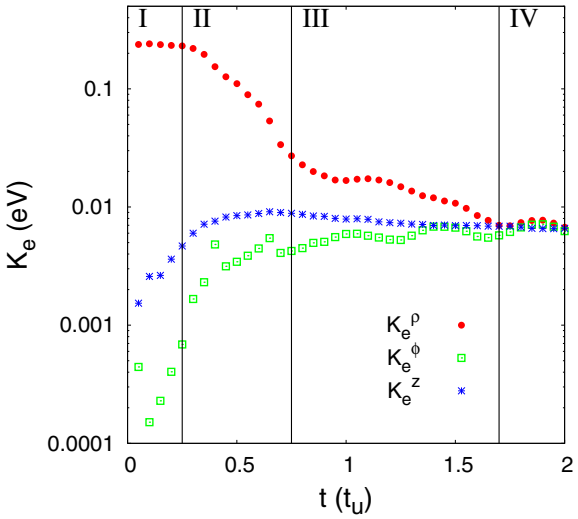

Fig. 2. (Color online) Radial, lateral, and vertical components of the average kinetic energy of the electrons (K_e^ρ, K_e^ϕ, and K_e^z) with initial excitation $Q_e = 80$ eV/Å. Four different stages of evolution are identified and discussed in the text.

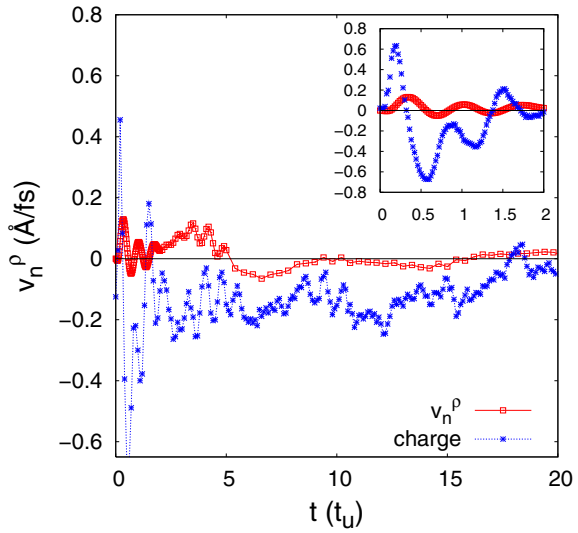

Fig. 3. (Color online) Radial velocity of the nuclei, v_n^ρ (red), in a cylindrical shell of inner and outer radii 5 Å and 10 Å, respectively, and net charge inside a cylinder of radius 5 Å (blue), as a function of time. The inset is a zoom on the first 2 t_u. These results are for $Q_e = 80$ eV/Å.

is after about 1.7 t_u. At this point, the electrons are locally in equilibrium and their velocities follow a Maxwell-Boltzmann distribution. However, the energy of the electrons which are closest to the trajectory of the ion is still larger than farther away, and this situation – the presence of a gradient in the electronic temperature profile – lasts for at least 20 t_u.

We plot in Figure 3 the radial component of the velocities of the nuclei in a cylindrical shell of inner and outer radii 5 and 10 Å, respectively, as well as the total effective charge on those nuclei as a function of time. In the

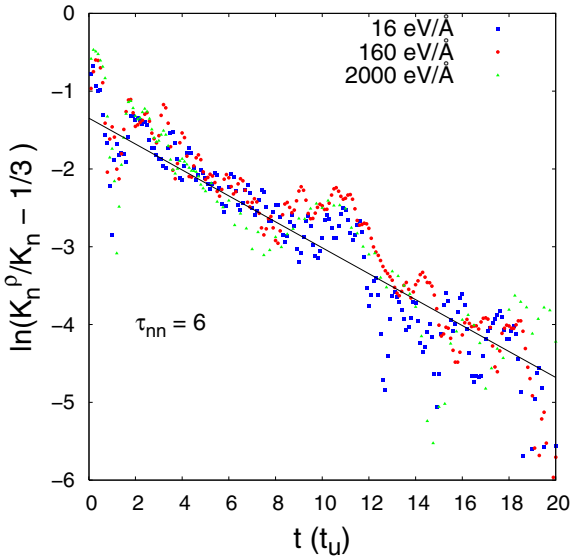

Fig. 4. (Color online) Linearized representations of the radial component of the kinetic energy of the nuclei, K_n^ρ, inside a cylinder of radius 15 Å, as a function of time. The straight line, which is a guide to the eye, is an exponentially-decreasing function with a characteristic time of 6 t_u.

early moments, the motion of the nuclei is strongly correlated to the motion of the electrons: the velocity of the nuclei reaches a peak at the moment the charge changes sign. As a result of this correlation, the nuclei, just as the electrons, develop a strong radial velocity. The thermal relaxation of the nuclei is illustrated in Figure 4 for all atoms within a 15 Å cylinder centered on the impact trajectory, for three different values of the stopping power; the radial component of the kinetic energy of the nuclei, K_n^ρ, is normalized by the total kinetic energy (i.e., the sum of all three components). The three curves are well represented by an exponentially decreasing function of time that converges to 1/3, with a relaxation time of about 6 t_u, as indicated by the straight line in Figure 4. Thus the radial velocity dominates the other two components for a period of about 6 t_u, after which equilibrium between all three components is attained.

The amplitude of the deformations in the system can be measured by examining the displacements of the nuclei as a function of time. We plot in Figure 5 the root mean square displacements of the nuclei ($\overline{\Delta r}$) for several 5-Å thick cylindrical shells centered on the impact trajectory, as a function of time. For all shells, $\overline{\Delta r}$ increases with time, goes through a maximum, and tends to 0.2 Å, which corresponds to the equilibrium amplitude of vibration. The position of the maximum in the curves varies at a rate of about 2.2 Å/t_u, which corresponds to the speed of sound in the system. This is higher than typical values and is a direct consequence of the small mass of the nuclei we imposed. We have calculated the pressure in the system and found it to follow precisely the motion of the displacement amplitude. Thus, the ion impact causes a pressure wave to develop, which proceeds outward from the center.

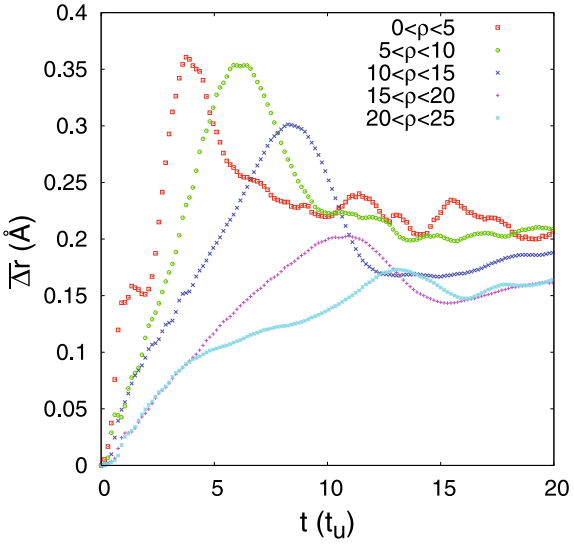

Fig. 5. (Color online) Root mean square displacements of the nuclei, $\overline{\Delta r}$, for different cylindrical shells centered on the impact trajectory, as a function of time. These results are for $Q_e = 80$ eV/Å.

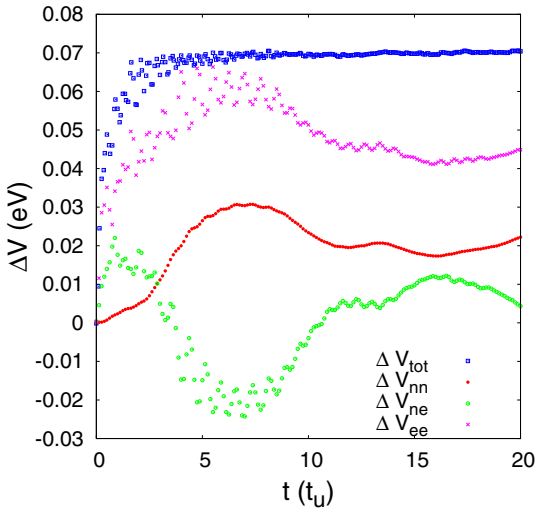

Fig. 6. (Color online) Total potential energy of the system, $\Delta V_{\rm tot}$, as well as individual components, ΔV_{nn}, ΔV_{ne}, and ΔV_{ee}, as a function of time for an initial excitation $Q_e = 80$ eV/Å.

To complete this description, we present in Figure 6 the evolution in time of the total potential energy of the system ($\Delta V_{\rm tot}$), as well as the individual components (ΔV_{nn}, ΔV_{ne}, and ΔV_{ee}). We find that the total potential energy converges rapidly – within about 2 t_u – to a value higher than equilibrium: because of the increased temperature, the spatial degrees of freedom acquire some energy during this time. As there are no fluctuations afterwards, it can be inferred that the ionised track has vanished at this point, which also corresponds to the timescale for electronic thermal relaxation as we saw above. From these observations, we conclude that Coulombic energy-transfer processes occur on a timescale shorter than 2 t_u; this will be important for the discussion that follows.

4.2 Energy transfer mechanisms

We have tried to analyze our results in terms of the models discussed earlier – Coulomb explosion and thermal transfer – and found that neither could explain the data over the whole period of time, from the ion impact to the complete thermalization of the system. We note in particular that, with average atomic displacements of no more than a fraction of an Å (cf. Fig. 5), one can hardly speak of a Coulomb explosion. In fact, our calculations suggest that the energy transfer from the ion to the lattice proceeds over three distinct phases. First, the electrons move towards the center where a net negative charge develops; this causes the nuclei to also be attracted towards the center, i.e., they acquire a negative radial velocity, and this lasts for about 0.1 t_u. Second, the electrons move away from the impact trajectory, which induces a positive charge in the central region; the nuclei thus feel a Coulomb repulsion, causing an outward radial velocity to develop. This process takes place with a characteristic timescale of about 2 t_u and operates for about 6 t_u. Third, and finally, the electrons attain local equilibrium so that the net charge along the ion trajectory vanishes; at this point, the transfer of energy to the nuclei occurs by random collisions, i.e., Coulomb processes are over.

We describe the energy transfer mechanisms in more detail in the following sections. The first two processes are both Coulombic and are discussed together. We note that the pressure wave brings about no energy transfer between electrons and nuclei – it involves the nuclei alone.

4.2.1 Coulomb processes

The initial gain in kinetic energy of the nuclei – first attracted towards the center then pushed away – derives entirely from Coulomb interactions. Since neither process results in significant displacements of the atoms, the concept of Coulomb explosion is not relevant; it is more appropriate to refer to this phase as Coulomb heating.

We plot in Figure 7a the evolution in time of the kinetic energy of the nuclei for three different values of the stopping power – panels (b) and (c) zoom on the very short (0–0.5 t_u) and the intermediate (0–2 t_u) time windows, respectively, during which the first two energy-transfer mechanisms take place. The peaks, marked by the horizontal lines, indicate the times at which the energy-transfer mechanisms start to slow down.

The first peak occurs at the moment when the electrons escape from the center and the charge in the central region changes sign (cf. Fig. 3). We plot the peak values K_{n1} as a function of the initial energy deposition in the system, Q_e, in Figure 8. We observe that the height of the first peak decreases with increasing ion energy. This is a clear indication that the process giving rise to this peak is of Coulomb origin, more precisely it results from the

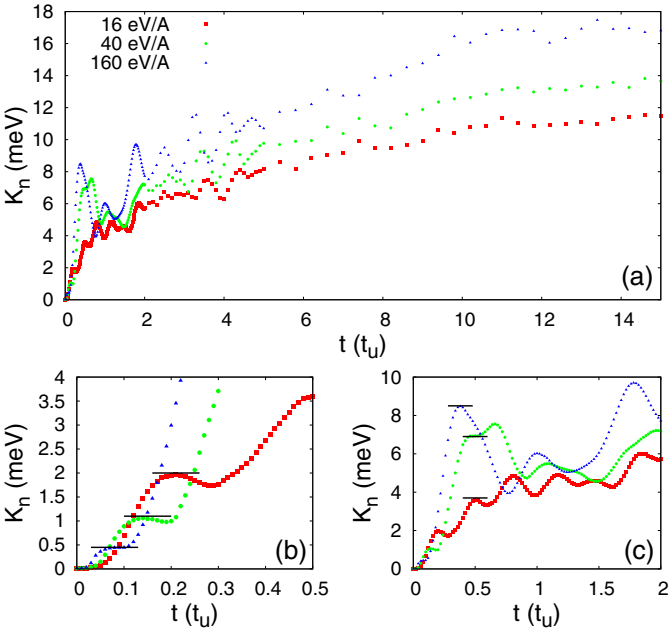

Fig. 7. (Color online) Kinetic energy of the nuclei, K_n, in a cylinder of radius 15 Å for three different levels of excitation Q_e as a function of time. The horizontal bars indicate the end of the two Coulomb heating phases for each value of the stopping power.

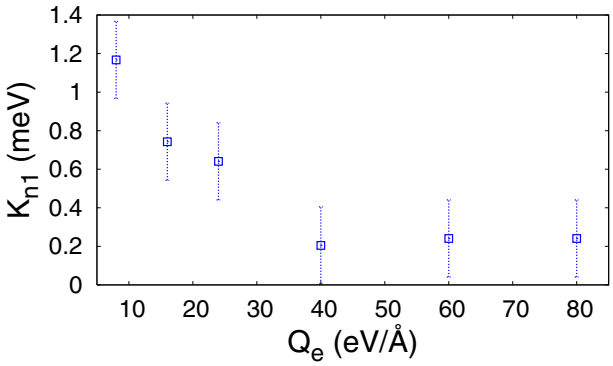

Fig. 8. (Color online) Kinetic energy of the nuclei at the first maximum, K_{n1}, as a function of the stopping power Q_e.

presence of electrons near the impact trajectory. Indeed, the higher the energy of the ion, the larger the velocities of the electrons and thus the less time they spend in this region (viz., inversely proportional to velocity).

The second peak occurs when the "outbound" radial motion is slowed down by the attractive interaction of the lattice. If the second energy-transfer phase indeed arises from Coulomb repulsion, then the kinetic energy of the nuclei at the second maximum, K_{n2}, should be proportional to the charge in the central region along the impact trajectory. In our model, this charge is in fact proportional to the number of PEs captured at the boundaries. We show in Figure 9 that this relation is indeed verified.

Taken together with the correlation between the charge and the velocity of the nuclei (Fig. 3), those relations clearly establish that the early phases of energy transfer from the electrons to the atoms arises from Coulomb processes. These operate on a timescale of about 2 t_u; a thermal transfer regime then takes over as we demonstrate next.

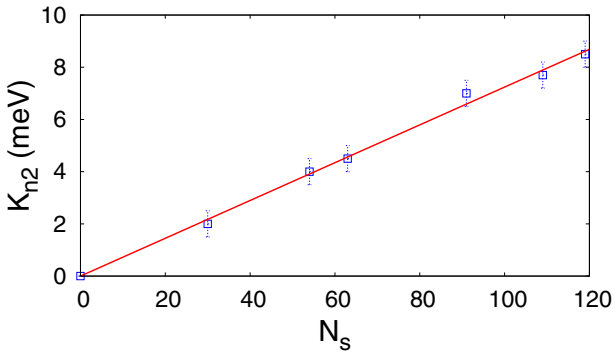

Fig. 9. (Color online) Kinetic energy of the nuclei at the second maximum, K_{n2}, as a function of the number of PEs N_s stopped at boundaries, i.e., for different values of Q_e. The straight line, which is a guide to the eye, shows that the process arises from Coulomb repulsion.

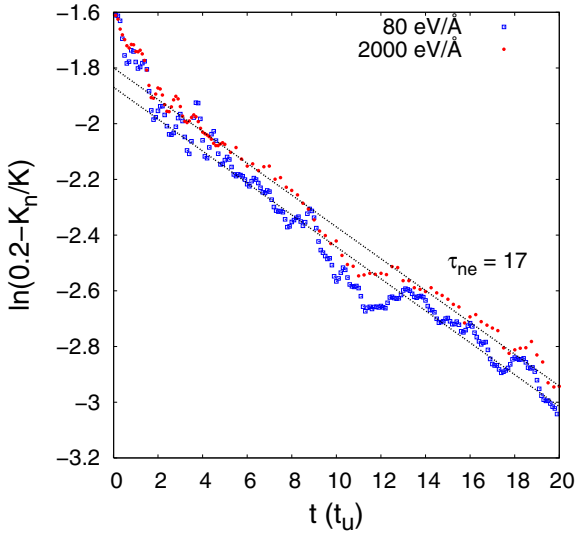

Fig. 10. (Color online) Linear representation of the kinetic energy of the nuclei, K_n, as a function of time, for two values of the stopping power. The equilibration process is well represented by an exponential function with a characteristic time of 17 t_u, as shown.

4.2.2 Thermal transfer

As discussed earlier, the electron gas and the total potential energy of the whole system exhibit local thermal equilibrium properties after about 2 t_u. Except for the large radial velocity component, the nuclei also show equilibrium. Thus, as of this time, the average kinetic energy of the nuclei, $\overline{K_n}$, should evolve according to equation (6), which derives from the "thermal spike" model. To demonstrate this, we plot in Figure 10 the evolution in time of the nuclear kinetic energy in a cylindrical region of radius 15 Å. More precisely, we consider the quantity K_n/K

(where K is the total kinetic energy) which behaves as $\overline{K}_n$ if the heat flow out of the considered region is small compared to the energy transfer from the electrons. In a state of complete thermal equilibrium, the temperatures of the electrons and the nuclei are equal, and each carries a portion $1/(N+1)$ of the total kinetic energy, with N the number of PEs per atom; here $N = 4$ so that the kinetic energy contributions should average 1/5 in equilibrium. Figure 10 shows that, indeed, K_n/K tends to 1/5.

The characteristic time can be calculated by fitting the data points to an exponential function, yielding $\tau_{ne} = 17$ t_u; this is also shown in Figure 10 where an exponential behaviour is clearly visible past the first 2 t_u, which corresponds to the end of the Coulomb regime. (Note that the variations in this regime appear smaller because of the use of a log scale; likewise, the variations further down in time are normal statistical fluctuations.) The value of τ_{ne} we find is slightly larger than the expected value of 13 t_u mentioned earlier. The difference is due to the fact that we neglect here the diffusion of energy which, if taken into account, would necessarily lead to a shorter relaxation time.

To summarize, the transfer of energy from the impact zone to the nuclei occurs initially through Coulomb processes. The charge-velocity correlation and the potential energy variations indicate that the timescale for this phase is about 2 t_u. Thermal processes take over on longer timescales and equilibrium is reached in 15–20 t_u. This phase is well described by linear transport theory. A transition regime where both coexist is possible between 1 and 2 t_u. These values are order-of-magnitude estimates for a "generic material"; evidently, the precise numbers will depend on the specific ions and materials under study.

4.2.3 Discussion

According to our model, the transfer of energy from the impact trajectory to the nuclei occurs initially through Coulomb heating, then via random collisions, i.e., a thermal process. A number of simplifying assumptions have been effected in order to reduce the computational load (i.e., to make the problem tractable); we discuss here the impact of those simplifications.

To speed up the dynamics, which is dominated by the electrons, the mass of the ions was set to 0.01 amu. We found that the Coulomb heating phase lasts at most 2 t_u, and that the atomic displacements induced by this mechanism are less than interatomic distances. Increasing the mass of the ion cores to larger values is unlikely to decrease the role of Coulomb effects. There might be some effects on the numerical value of the timescale for the transfer of energy to the ions, but large changes in the transition time and relative importance of the Coulomb heating and thermal transfer phases are not expected since these depend on the electrons dynamics only.

On the basis of our CASP calculations, we have considered that only weakly bound electrons were affected by the swift ion. Core electrons, which are closer to the nucleus, cannot be accounted for with the forces we used here. (A Monte Carlo procedure should be used to this end [25].) Thus, interactions between fast electrons and core electrons, such as Auger-like processes, are excluded, i.e., the efficiency of the fast electrons to carry energy away from the ion track is overestimated a bit. Likewise, screening is smaller than would be the case if inner-shell electrons were considered. Thus, in effect, the timescales quoted above are upper bounds to the real values.

In spite of the considerable simplifications made in our model, it is found that our "pseudo-electron" approach leads to physically correct results. This method, however, remains to be validated in more realistic materials before it can be applied to other interesting problems such as the origin of residual structural damage (i.e., atomic displacements) along the ion trajectory or implemented in a complete Monte Carlo simulator engine encompassing all relevant time scales.

5 Conclusion

In conclusion, we have studied in silico the sequence of mechanisms involved in the energy loss of the energetic electrons left in the wake of a swift heavy ion traversing a generic solid target. The electron density was represented by pseudo-electrons which were followed by molecular dynamics, allowing the energy transfer from electrons to ions to be studied without having to rely on equilibrium electron-phonon coupling constants. We find that during the first 2 t_u – a t_u is about a picosecond –, electrons initially become concentrated at the center of the ion track and then altogether rapidly leave this region. A large fraction of the energetic electrons travel several nm's from the ion track centre before they start to loose energy. The ions of the target lattice near the center of the ion track gain kinetic energy during this same period, through mutual Coulomb repulsion. The velocities of both electrons and ions are predominantly radial during this phase, and a shock wave is initiated which moves radially outward. We refer to this phase as Coulomb heating – the displacements of the ions is much less than an interatomic distance. After the first 2 t_u, two thermal processes set in: the velocities of ions become randomized (instead of predominantly radial) with a time constant of 6 t_u. Also, the energy transfer from the hot electrons to the ions proceeds and can be characterized as a purely thermal exchange with a characteristic time of 17 t_u. These results indicate that our approach, whereby the interaction between a large density of highly excited electrons and the ions on the atomic lattice is modeled by pseudo-electrons, is valid and should be expanded to more realistic systems.

This work has been supported by grants from the Natural Sciences and Engineering Research Council of Canada (NSERC) and the *Fonds Québécois de la Recherche sur la Nature et les Technologies* (FQRNT). We thank the *Réseau Québécois de Calcul de Haute Performance* (RQCHP) for generous allocations of computer resources.

References

1. G. Szenes, Z.E. Horváth, B. Pécz, F. Pászti, L. Tóth, Phys. Rev. B **65**, 045206 (2002)
2. O. Herre, W. Wesch, E. Wendler, P.I. Gaiduk, F.F. Komarov, S. Klaumünzer, P. Meier, Phys. Rev. B **58**, 4832 (1998)
3. A. Dunlop, G. Jaskierowicz, G. Rizza, M. Kopcewicz, Phys. Rev. Lett. **90**, 015503 (2003)
4. A. Kamarou, W. Wesch, E. Wendler, A. Undisz, A. Rettenmayr, Phys. Rev. B **73**, 184107 (2006)
5. J.F. Ziegler, *The stopping and range of ions in solids* (Pergamon Press, 1985)
6. E.M. Bringa, R.E. Johnson, Nucl. Instr. Meth. B **143**, 513 (1998)
7. E.M. Bringa, R.E. Johnson, L. Dutkiewicz, Nucl. Instr. Meth. B **152**, 267 (1999)
8. E.M. Bringa, R.E. Johnson, Phys. Rev. Lett. **88**, 165501 (2002)
9. R.L. Fleischer, P.B. Price, R.M. Walker, J. Appl. Phys. **36**, 3645 (1965)
10. M. Toulemonde, C. Dufour, E. Paumier, Phys. Rev. B **46**, 14362 (1992)
11. I.S. Bitensky, E.S. Parilis, Nucl. Instr. Meth. B **21**, 26 (1987)
12. P. Stampfli, Nucl. Instr. Meth. B **107**, 138 (1996)
13. S. Klaumünzer, G. Schumacher, Phys. Rev. Lett. **51**, 1987 (1983)
14. M. Chicoine, S. Roorda, L. Cliche, R.A. Masut, Phys. Rev. B **56**, 1551 (1997)
15. L. Cliche, S. Roorda, M. Chicoine, R.A. Masut, Phys. Rev. Lett. **75**, 2348 (1995)
16. *Ion Tracks in solids*, edited by R. Fleisher, Mater. Res. Soc. Bull. **20** (1995)
17. S. Roorda, T. van Dillen, A. Polman, C. Graf, A. van Blaaderen, B. Kooi, Adv. Mater. **16**, 235 (2004)
18. L. Tapasztó, G. Dobrik, P. Nemes-Incze, G. Vertesy, Ph. Lambin, L.P. Biró, Phys. Rev. B **78**, 233407 (2008)
19. D. Frenkel, B. Smit, *Understanding molecular simulation* (Academic Press, 2002), 2nd edn.
20. V. Mijoule, L.J. Lewis, M. Meunier, Phys. Rev. A **73**, 033203 (2006)
21. S.K. Ghosh, B.M. Deb, Phys. Rep. **92**, 1 (1982)
22. C.J. Fennell, J.D. Gezelter, J. Chem. Phys. **124**, 234104 (2006)
23. P.L. Grande, G. Schiwietz, Phys. Rev. A **58**, 3796 (1998)
24. P.L. Grande, G. Schiwietz, Nucl. Instr. Meth. B **195**, 55 (2002)
25. T. Ditmire, T. Donnelly, A.M. Rubenchik, R.W. Falcone, M.D. Perry, Phys. Rev. A **53**, 3379 (1996)